A Study of Laminar Separation Bubble in the Concave Region of an Airfoil Using Laser Velocimetry

Sivaramakrishnan Mangalam
Analytical Services & Materials, Inc.
Tabb, Virginia

and

James F. Meyers
John R. Dagenhart
William D. Harvey
NASA Langley Research Center
Hampton, Virginia

Symposium on Laser Anemometry
ASME 1985 Winter Annual Meeting
November 17-21, 1985
Miami, Florida

A Study of Laminar Separation Bubble in the Concave Region of an Airfoil Using Laser Velocimetry

by

Sivaramakrishnan Mangalam
Analytical Services & Materials, Inc.
Tabb, Virginia

and

James F. Meyers
John R. Dagenhart
William D. Harvey
NASA Langley Research Center
Hampton, Virginia

Abstract

Laser velocimetry (LV) was used to study the nature of laminar separation bubbles in the concave region of a 1.83-meter airfoil model which was tested in the NASA Langley Low Turbulence Pressure Tunnel. Three component, coincident data from LV measurements including histograms of particle velocity, mean velocity profiles, turbulence intensity, and Reynolds stresses within the shear layer were used to determine the locations of laminar separation, transition, and turbulent reattachment. Boundary-layer parameters determined from velocity profiles were used to compare the results with existing empirical relations for describing the laminar separation bubble.

Nomenclature

B	van Ingen parameter (Equation 3)
C	Horton parameter (Equation 2)
c	airfoil chord, m
$C_p \quad \frac{p \quad p}{0.5 \quad \rho U^{2}}$	pressure coefficient

H_{12}	$\frac{\delta^*}{\theta}$	shape factor
H_{32}	$\frac{\delta_3}{\theta}$	shape factor
p		static pressure, N/m^2
R_c		chord Reynolds number
U		streamwise velocity component, m/sec
U_e		edge velocity, m/sec
U_R		edge velocity at reattachment, m/sec
U_s		edge velocity at separation, m/sec
$U_{à}$		free stream velocity, m/sec
V		normal velocity component, m/sec
X		chordwise distance from the leading edge, m
X_{tr}		distance between transition location and laminar separation point, cm
Y		distance normal to the model surface, cm
γ		angle made by dividing streamline (Equation 3), deg
δ		boundary-layer thickness, cm
δ^*		displacement thickness, cm
δ_3		energy thickness, cm
ρ		air density, kg/m3
σ		Crabtree parameter (Equation 1)
θ		momentum thickness, cm

Introduction

The leading edge separation bubble on an airfoil is formed when the laminar boundary layer separates from the surface as a result of the strong adverse pressure gradient downstream of minimum pressure. The separated shear layer, like free shear layer jets and wakes, is very unstable and hence transition occurs within a short distance downstream of separation. There is very little diffusion in the laminar part of the separated region but downstream of transition, rapid entrainment from the external stream due to turbulent shear stresses energizes the shear layer. Under suitable geometric and flow conditions, reattachment occurs, resulting in what is generally known as a separation bubble. A sketch of a laminar separation bubble is shown in Figure 1 where S is the point of laminar separation, T is the transition location, and R is the location of turbulent reattachment. In view of the presence of reverse flow and entrainment within the bubble it is possible to divide the bubble into two regions, the lower region close to the surface in which the flow is predominantly against the stream direction (reverse flow) and the upper region where the flow is in the flow direction (entrainment). These two regions are split by a zero mean velocity dividing line o-o (see Figure 1).

B. M. Jones, reference 1, was perhaps the first to study separation bubbles. He observed the existence of separation and reattachment of the boundary layer over cambered airfoils. The structure and behavior of laminar separation bubbles were studied on a flat plate by Gaster, reference 2. An adverse pressure gradient on the flat plate was induced by mounting a small auxiliary airfoil in its inverted position above the flat plate. An excellent review of early experimental and theoretical work on laminar separation bubbles can be found in reference 3 and subsequent reviews of pertinent literature can be found in references 4 and 5. Almost all previous experiments on transition in separated shear layer have been performed on either backward facing steps or axisymmetric jets, reference 5. Flow separation in these cases is forced by an abrupt change in geometry whereas in almost all practical situations separation is brought about by a strong adverse pressure gradient along a smooth surface. It is clear that while there must be some similarities in the characteristics of the bubble in all these cases, there must also be significant differences. An experiment was recently conducted in the NASA Langley Low-Turbulence Pressure Tunnel to obtain detailed information on the laminar separation bubble in the concave region of an airfoil using laser velocimetry. The present paper portrays the picture of the laminar separation bubble through the coincident data obtained with the three-component laser velocimeter system and provides quantitative information on the shape and size of the bubble, the length of the laminar and reattachment zones, and the location of transition and vigorous reverse flow regions.

Test Apparatus

A photograph of the 1.83-meter chord airfoil model tested in the NASA Langley Low-Turbulence Pressure Tunnel (LTPT) is shown in Figure 2. The view is of model upper surface and leading-edge region with spanwise suction strips. The model schematic diagram with inviscid pressure distribution is shown in Figure 3. The model consists of two parts a structural element and a test element. The test element consists of the leading edge and the upper surface back to midchord. The structural element consists of the spar and the remainder of the airfoil surface including the 10 percent chord trailing-edge flap which is used to adjust the location of the leading-edge stagnation point. The upper surface leading-edge region of this model closely resembles the lower-surface leading-edge of a possible advanced laminar-flow control supercritical airfoil, reference 6. The suction ports indicated in the sketch were used to insure attached flow in an experiment, reference 7, to study the formation and growth of Görtler vortices in the concave region but in the present experiment suction was turned off to induce flow separation in the compression zone of the concave region. The concave region on the airfoil upper surface (test region) begins at $x/c = 0.175$ and ends at $x/c = 0.275$. The compression (adverse pressure gradient) region extends from $x/c = 0.175$ to $x/c = 0.225$.

The LTPT is a pressurized, closed circuit, continuous flow wind tunnel. The test section is 2.29 m high, 2.29 m long, and 0.91 m wide. The tunnel has excellent flow qualities due, in part, to the nine screens in the settling chamber. The velocity fluctuations in the test section were measured to be 0.025 percent at 0.05 Mach number, reference 8, the speed at which the present experiment was conducted. The pressure fluctuations at the test section wall, normalized with respect to free-stream pressure were ~ 10-5 at this Mach number. The present experiment was conducted at atmospheric pressure. The chord Reynolds number was 2.1 million.

A specialized single axis three-component laser velocimeter was used to study the flow field in the test region (Figure 4). The single axis, five-beam optical configuration, reference 9, uses the standard two color, two-component beam pattern with the two green beams (514.5 nm) arranged in the horizontal plane and the two blue beams (488.0 nm) arranged in the vertical plane forming a diamond pattern to measure the streamwise component (U) (green beams) and the vertical component (V) (blue beams). A third green beam is placed along the optical axis bisecting the angle between the original two green beams. The addition of this beam creates two additional fringe patterns within the sample volume. These additional fringe patterns are inclined symmetrically about the optical axis yielding equal contributions of the U-component and equal but opposite contributions of the W-component (spanwise velocity component). The W velocity component is then obtained from the difference between the two signal frequencies. This is achieved by incorporating Bragg cells in the two outside beams to separate by frequency the three signals obtained from the three green fringe patterns. A filter network isolates the U component signal frequency and the two signal frequencies from the inclined fringe patterns which are then input to an electronic double balanced mixer. The lower frequency signal from the mixer is the frequency difference between the two input signals and is the W component signal frequency with a known bias depending on Bragg cell frequencies. The flow was seeded with tridecane particles using a particle generator located upstream of the screens. The three-component, coincident LV data were recorded and processed by a dedicated computer system. The results were later transformed to the model coordinate system for analysis.

Results and Discussion

The present experimental study was intended to obtain detailed information on the laminar-separation bubble characteristics in the concave region of the airfoil model. Histograms of particle velocity components at different heights above the model surface are shown in Figure 5 for a number of chord locations. These histograms vividly describe the nature of the flow in the boundary layer. In the presence of a laminar boundary layer the mean velocities have a small standard deviation and the plots have a typical single large peak. When the sample volume is in a transitory flow or in a turbulent boundary layer, the histograms of mean velocities exhibit a large spread (large standard deviation) and unlike hot-wire measurements, the reverse flow within the separated region is directly indicated by the presence of negative particle velocities. Thus a fairly clear picture of the separation bubble characteristics can be obtained by carefully studying the histograms. Histograms up to 19 percent chord have typical laminar particle velocity distribution and are not shown here. At 19.5 percent chord significant changes were observed in the histograms as the laser beam traversed across the boundary layer (Figure 5). The mean normal velocity component in the boundary layer is close to zero at $Y = 0.20$ cm, but when the sample volume is moved to $Y = 0.05$ cm, one can observe a number of particles with appreciable normal velocity (~ 1 m/s). The location of the first occurrence of such a phenomenon indicates that the sample volume may have just entered the separated zone. Similar histograms were observed further downstream to $x/c = 0.215$. The nature of histograms changed drastically at this chord location, even at a height of 0.4 cm from the surface (Figure 5), it is possible to observe not only a large spread in mean U-component but also significant negative particle velocities in the normal direction. As the sample volume is traversed closer to the surface ($Y = 0.1$ cm) the velocity spread in both U- and V-components is large, and there are a number of particles with negative streamwise velocity components. It is worth noting that the population of particles expressed in percent has also dropped significantly at this chord location. The large spread in the mean velocities is assumed to be due to shear-layer transition from laminar to turbulent flow and the presence of negative velocities within the separated zone indicates reverse flow in the bubble. This behavior is more pronounced at 22-percent chord and the spread in the histograms, indicating turbulent flow, grows rapidly as x/c is increased to 23–percent chord. At 23-percent chord it is observed that the number of particles with negative streamwise velocity is negligible even at $Y = 0.05$ cm indicating that there is negligible reverse flow within the boundary layer at this location, i.e., the boundary layer is close to reattachment to the airfoil model surface. A completely reattached, turbulent boundary layer is indicated by histograms at 25-percent chord. Here there are no particles with negative velocity in the streamwise direction even at $Y = 0.04$ cm while the histograms have a large spread in particle velocity. The histograms of the magnitude and direction of the velocity vector within the boundary layer were also analyzed to determine the characteristics of the separation bubble. Histograms at two different heights at 21.5-percent chord and at 22–percent chord (Figure 6) clearly show that the particle flow angle covers the whole range of -180 deg to +180 deg near the surface and this combined with the large spread in the particle velocity distribution indicate that transition and large flow reversals occur in this region. The picture that emerges from a study of histograms is as follows.

The boundary layer is laminar and attached up to 19-percent chord and transition in the separated region occurring at about 21.5-percent chord. Reverse flow is noticeable at a height of 0.05 cm above the model surface from about 21.5-percent chord to 22.5percent chord. The reverse flow is most pronounced at x/c = 22.5-percent chord but is practically absent by 23-percent chord and hence the boundary layer is close to reattachment at 23-percent chord. There is no reverse flow at 23.5-percent chord and reattachment is complete. The boundary layer is fully turbulent downstream of this location.

The above qualitative description of the laminar separation bubble is supported by the chordwise variations in the boundary-layer profiles of mean streamwise velocity (Figure 7) and turbulence intensity

(Figure 8). Velocity profiles indicate separation of 0.19C and reattachment around 0.23C. Fully turbulent profile is observed at 0.25C. Largest fluctuations in turbulence intensity indicating the end of transition are observed at 0.225C.

In order to compare these results with existing prediction techniques for laminar separation bubble, boundary-layer thickness parameters δ^*, θ, δ_3, and shape factors H_{12} and H_{32} were determined from the mean streamwise velocity profiles. Laminar separation is generally known to occur where H_{32} goes below 1.515, reference 9, (σ in Figure 9). H_{32} remains below this value up to 0.215C where it begins to increase rapidly, indicating transition. The predicted value of H_{32} for a turbulent boundary layer is about 1.77 which is attained at $x/c = 0.235$. The shape factor H_{12} decreases marginally towards the point of separation and drops rapidly at transition from a maximum of about 4.91 at 0.215 chord to 1.54 at 0.23 chord.

Abrupt increase in momentum thickness θ, energy thickness δ_3 is observed at $x/c = 0.22$ indicating transition to turbulence (see Figure 10). The maximum value of the displacement thickness δ^* occurs at 0.21C indicating that the hump in the flow due to the separation bubble attains its maximum value just ahead of the transition.

A number of empirical relations have been suggested in literature, reference 11, to predict laminar separation bubble characteristics. According to Crabtree, reference 12, the parameter

$$\sigma \quad 1 \quad \frac{U_R}{U_S}{}^{2} \tag{1}$$

is of the order of 0.35 for a short bubble. The value of σ in the present experiment is 0.3634. According to Horton, reference 12, the transition in the separated shear layer occurs when

$$\frac{x_{tr}}{\theta_{sep}} \quad C\,\frac{10^{4}}{R_{\theta_{sep}}} \tag{2}$$

with values of C ranging from 3 to 5 (x_{tr} is the distance measured from the point of separation). This essentially means that Reynolds number based on and external flow velocity at separation is of the order of 30,000-40,000. In the present case $C = 4.6$ if x_{tr} is based on the beginning of transition. However, if x_{tr} corresponds to the end of transitions, C assumes a value of 6.9. It is speculated that the relatively higher value of transition Reynolds number in the shear layer may be due to the very low turbulence level in the wind tunnel.

In addition to the above laser velocimeter measurements, simultaneous observations of the number of particles in the sample volume were also made as the sample volume was traversed towards the surface. A significant, sharp drop in the number of particles in the sample volume was observed at a particular height above the surface. The very drastic decrease in the number of particles in the sample volume is attributed to the entrance of the sample volume into the separation bubble (the drop in the number of particles in the sample volume was significantly higher than the usual drop associated with the approach of the low velocity region near the surface). The approximate normal coordinate of this occurrence were noted in the test log book and the locus of these points (Figure 11, line L-L) approximates the laminar dividing streamline.

According to van Ingen, reference 11, the separation streamline leaving the wall at an angle γ (Figure 1) is given by

$$\tan \gamma \quad \frac{B}{R_{\theta_{sep}}} \tag{3}$$

with a value for the constant B of about 15 to 20. If the sudden drop in the number of particles in the sample volume is used as a criterion to define the separating streamline, we get a value of $B = 20.38$ with $\gamma = 1.56^{\circ}$.

Thus, the combined observations including histograms of velocity components and their flow angles, boundary-layer velocity profiles, turbulence intensity measurements, Reynolds stresses, and indications of the number of particles in the sample volume suggest the following picture of the separation bubble along the concave region of the airfoil model.

Laminar separation occurs near 19-percent chord, with shear-layer transition occurring between $x/c = 0.215$ and 0.22. Turbulent reattachment takes place at 0.235 chord. The maximum height of the laminar separation bubble is 4 mm ($\sim$ 0.22percent chord). The length of the laminar region of the bubble is 3-percent chord whereas transition and turbulent reattachment are completed within a distance of 1.5–percent chord.

Summary

Laser velocimeter measurements were made in the boundary layer along the concave region of an airfoil model to study the characteristics of the laminar separation bubble. Histograms of velocity components and the flow angularities, mean velocity profiles, turbulence intensities, and observations of the number of particles in the sample volume at different heights above the model surface and at a number of chord locations were used to describe the laminar separation bubble. A clear picture of the extent of the laminar region, the locations of transition, reverse flow regions, and the turbulent reattachment zone is obtained. These observations are supported by chordwise variation of boundary-layer parameters determined from mean velocity profiles. A comparison of test results with existing empirical relations shows good agreement. The present experiment on an airfoil model indicates that laser velocimetry is a very powerful tool to study the laminar separation bubble characteristics.

Acknowledgments

The authors wish to sincerely thank T. E. Hepner who was primarily responsible for making the laser velocimeter measurements in the experiment.

References

1. Jones, B. M.: *An Experimental Study of the Stalling of Wings*, NACA Reports & Memoranda No. 1588, December 1933.

2. Gaster, M.: *The Structure and Behavior of Laminar Separation Bubbles*, ARC R&M No. 3595, 1969.

3. Ward, J. W.: *The Behavior and Effects of Laminar Separation Bubbles on Aerofoils in Incompressible Flow*, J. Roy. Aero. Soc., Vol. 67, December 1963.

4. Tani, I.: *Low-Speed Flows Involving Bubble Separation*, Prog. Aeronautical Sciences, Vol. 5, 1974.

5. Mueller, T. J.: *Low Reynolds Number Vehicles*, AGARDograph AG-288, 1984.

6. Harvey, W. D.; and Pride, J. D.: *The NASA Langley Laminar Flow Control Airfoil Experiment*, AIAA Paper No. 82-0567, 12th AIAA Aerodynamics Testing Conference, Williamsburg, Virginia, March 1984.

7. Mangalam, S. M.; Dagenhart, J. R.; Hepner, T. E.; and Meyers, J. F.: *The Görtler Instability on an Airfoil*, AIAA 23rd Aerospace Sciences Meeting, Reno, Nevada, January 1985.

8. Stainback, P. C.; and Owen, F. K.: *Dynamic Flow Quality Measurements in the Langley Low Turbulence Pressure Tunnel*, Paper No. 84-0621, AIAA 13th Aerodynamic Testing Conference, San Diego, CA, March 1984.

9. Meyers, J. F.; and Hepner, T. E.: *Velocity Vector Analysis of a Juncture Flow Using a Three-Component Laser Velocimeter*, Second International Symposium on Applications of Laser Anemometry to Fluid Mechanics, July 2-4, 1984, Lisbon, Portugal.

10. Eppler, R.; and Somers, D. M.: *Airfoil Design for Reynolds Numbers Between 50,000 and 500,000*, Proceedings of the Conference on Low Reynolds Number Airfoil Aerodynamics, Notre Dame, Indiana, June 1985.

11. van Ingen, J. L.; and Boermans, L. M. M.: *Research on Laminar Separation Bubbles at Delft University of Technology in Relation to Low Reynolds Number Airfoil Aerodynamics*, Proceedings of the Conference on Low Reynolds Number Airfoil Aerodynamics, Notre Dame, Indiana, June 1985.

12. Crabtree, L. F.: *The Formation of Separated Flow on Wing Surfaces*, R and M 3122, 1959.

13. Horton, H. P.: *A Semi-empirical Theory for the Growth of Laminar Separation Bubbles*, ARC-CP 1073, 1967.

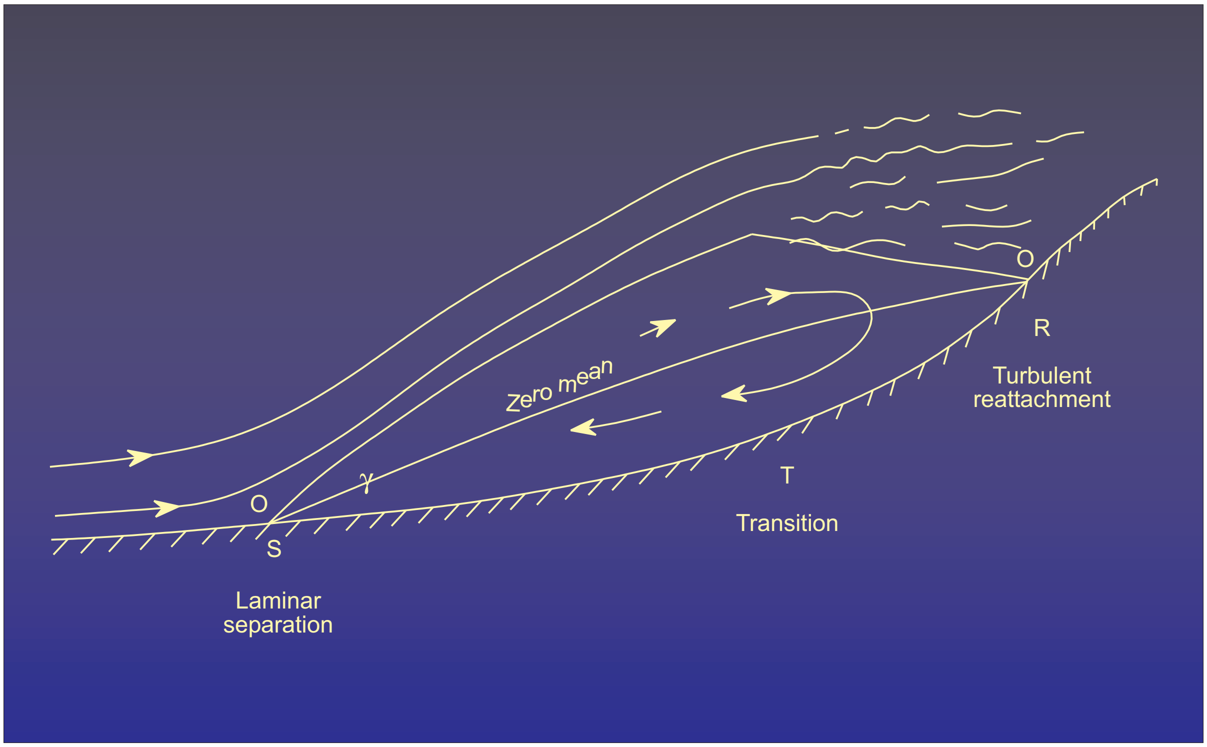

Figure 1. Schematic diagram of laminar separation bubble. (not to scale)

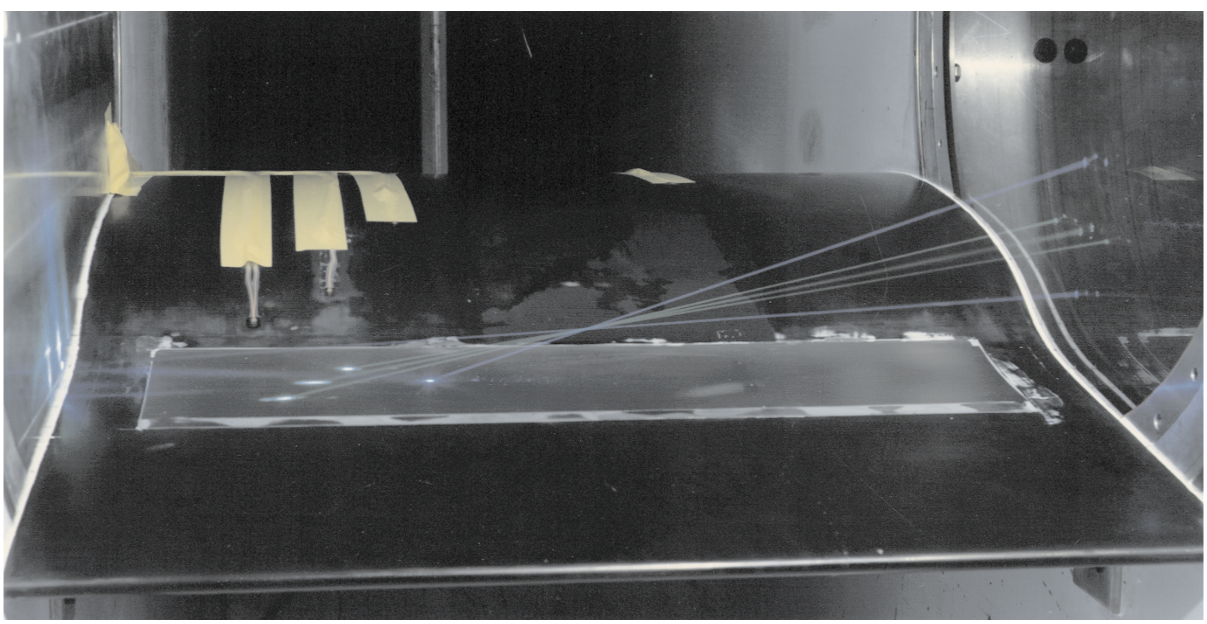

Figure 2. Airfoil model in LTPT.

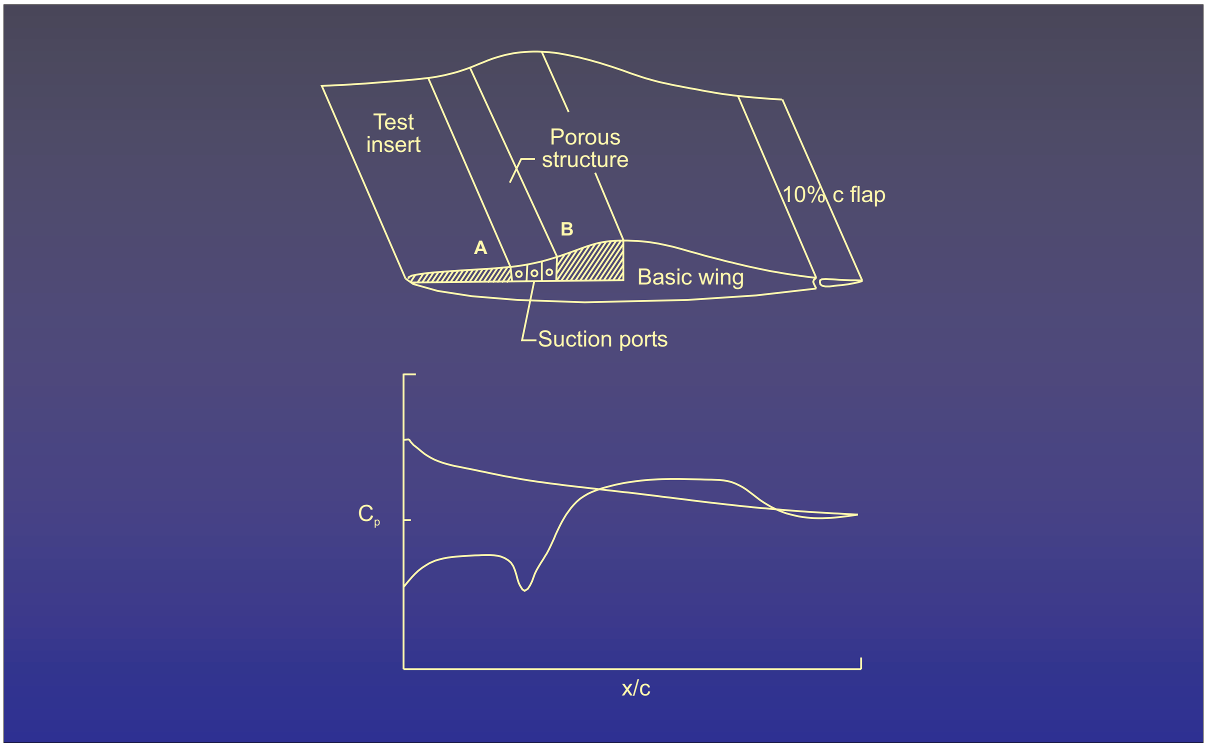

Figure 3. Model schematic diagram and C_p - *distribution*.

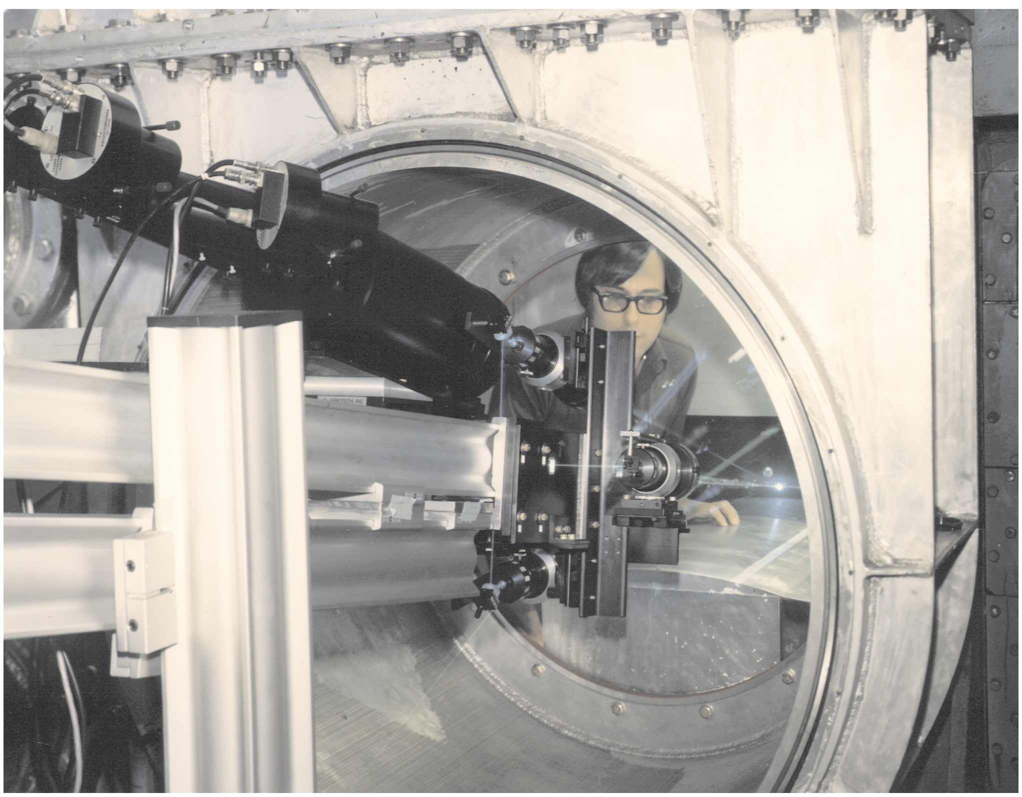

Figure 4. Laser optics.

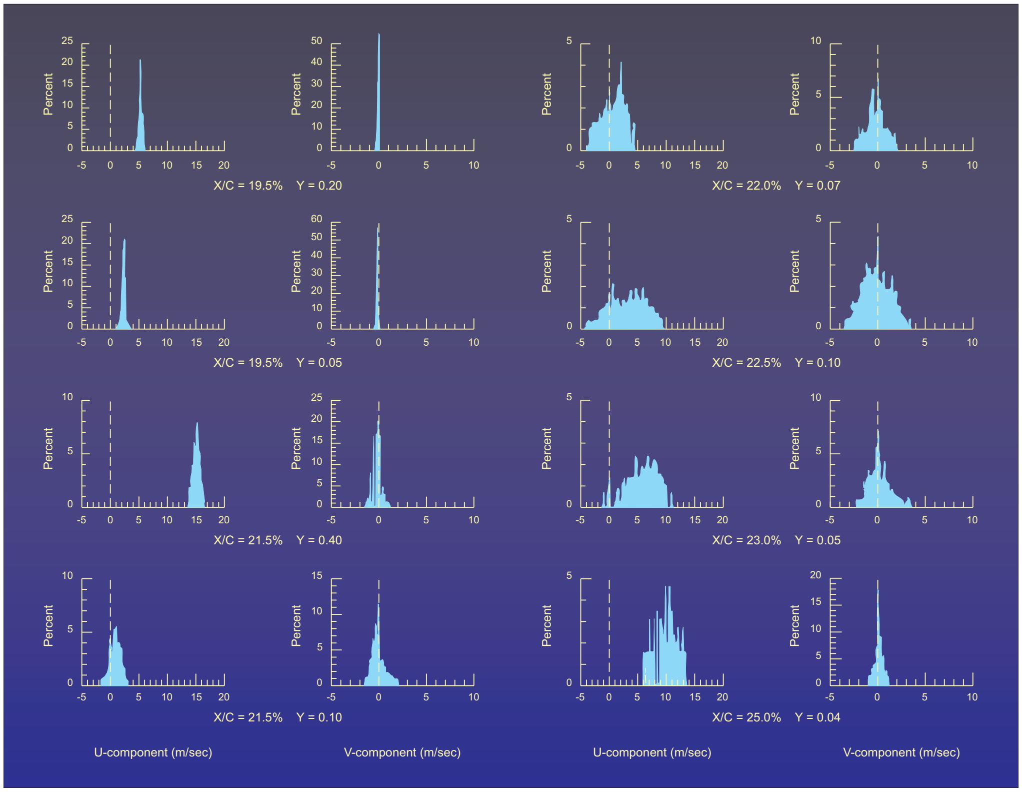

Figure 5. Histograms of streamwise and normal velocity components.

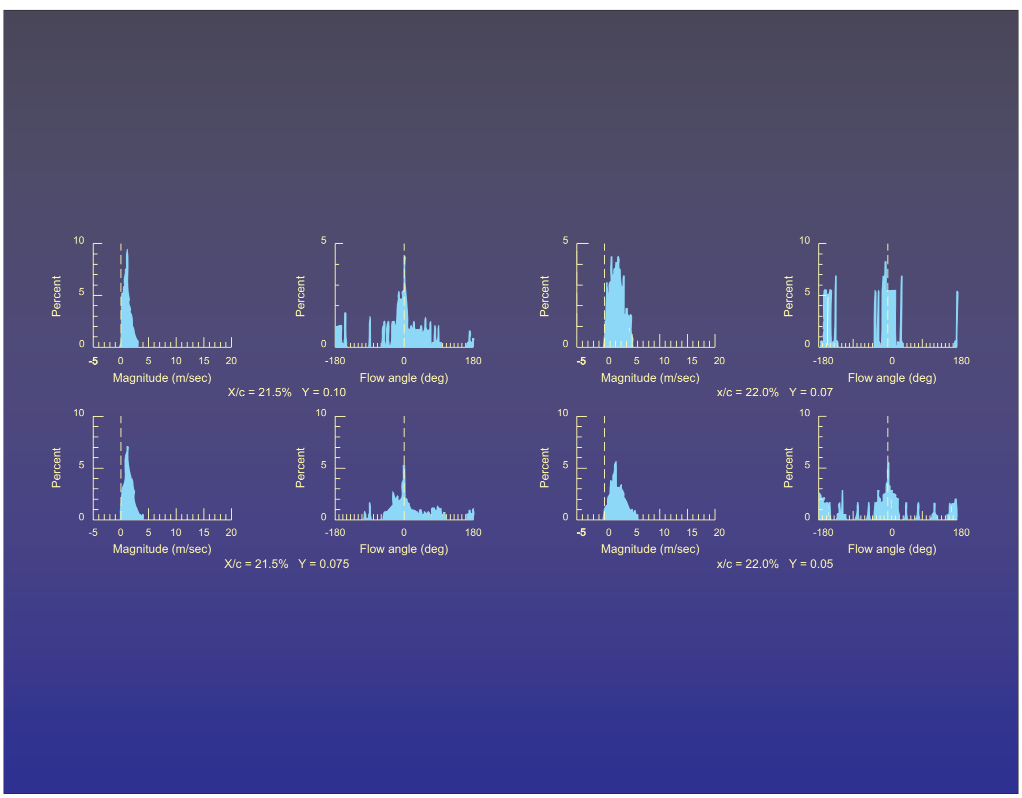

Figure 6. Histograms of resultant velocity and flow angle.

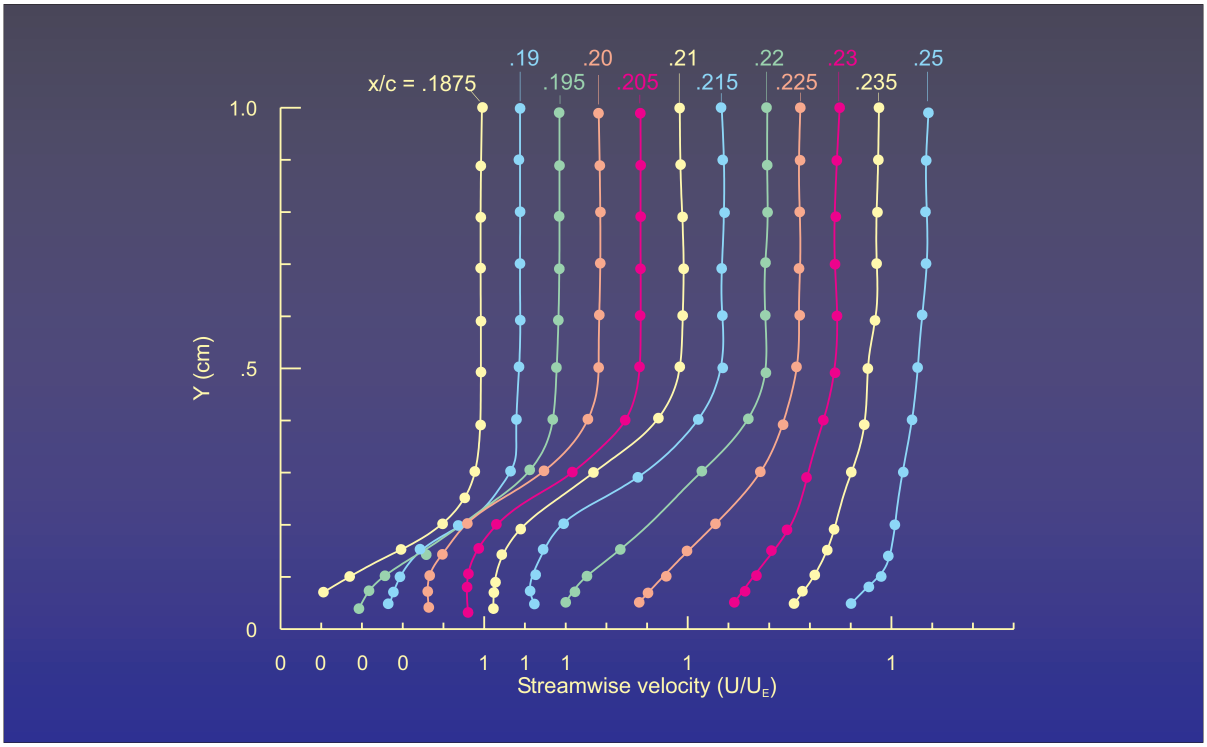

Figure 7. Chordwise variation in boundary-layer velocity profiles.

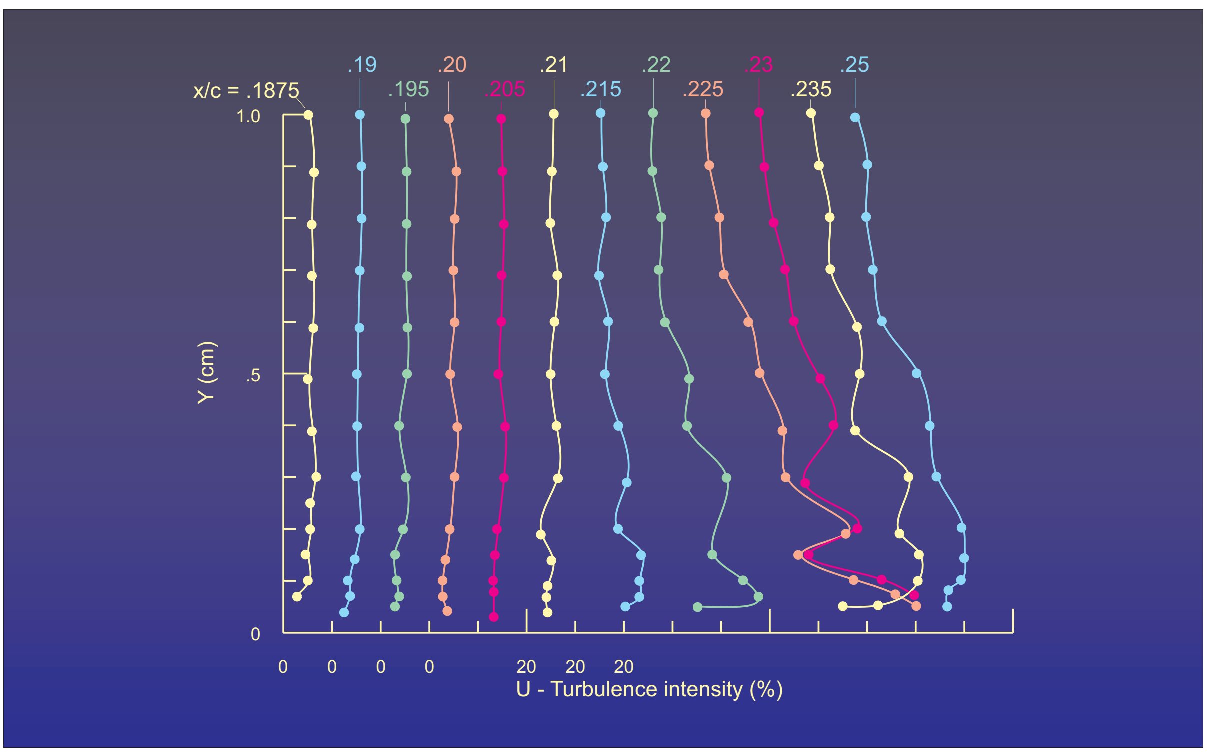

Figure 8. Chordwise variation in turbulence intensity of streamwise velocity component.

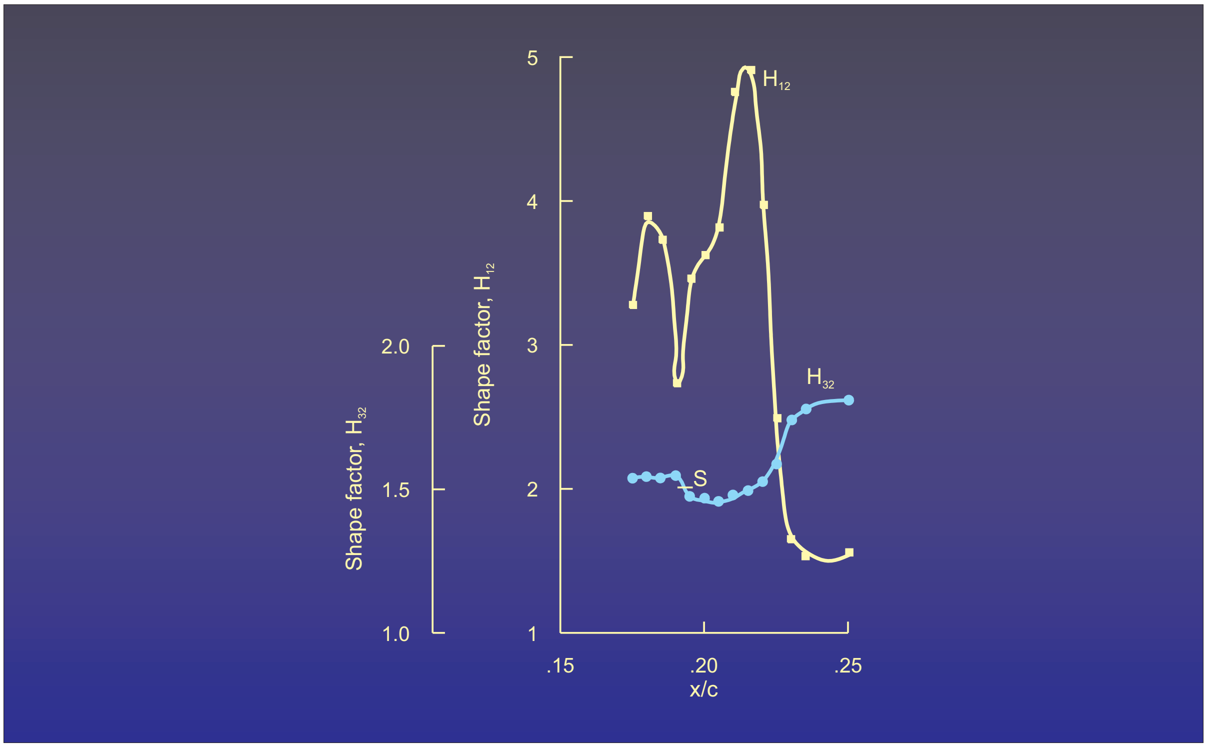

Figure 9. Chordwise variation in shape factors.

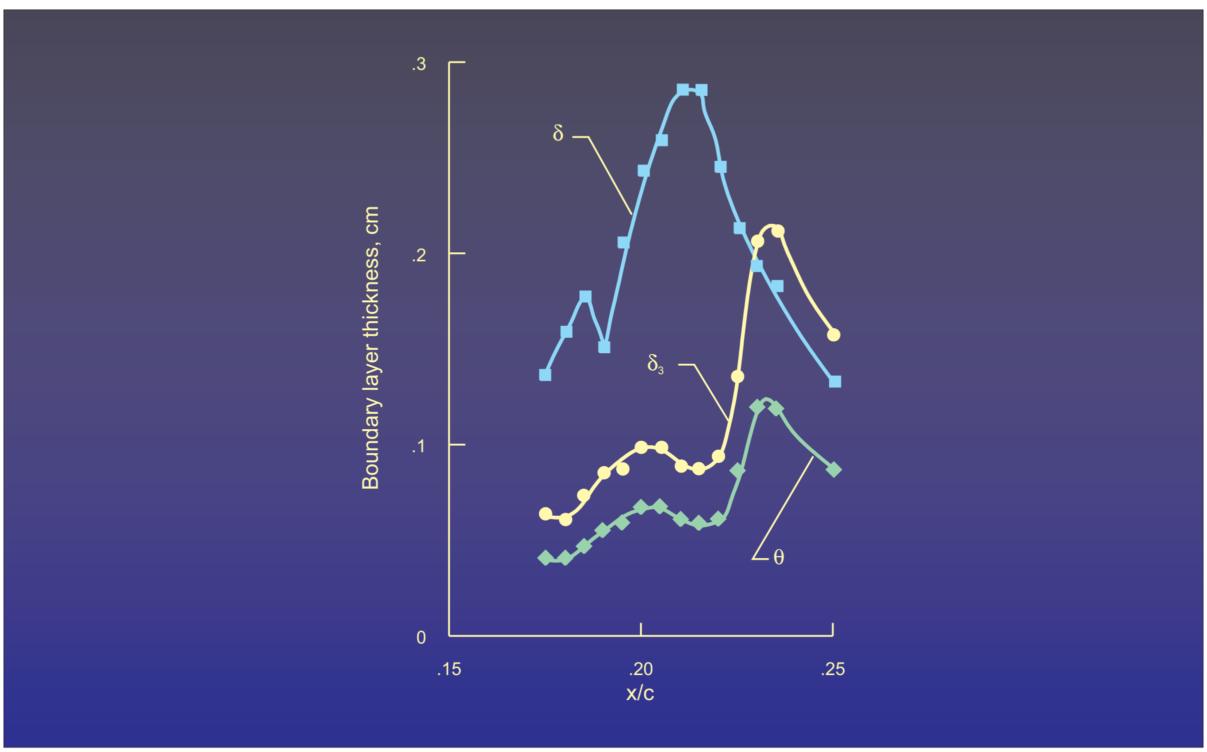

Figure 10. Chordwise variation in boundary-layer thickness.

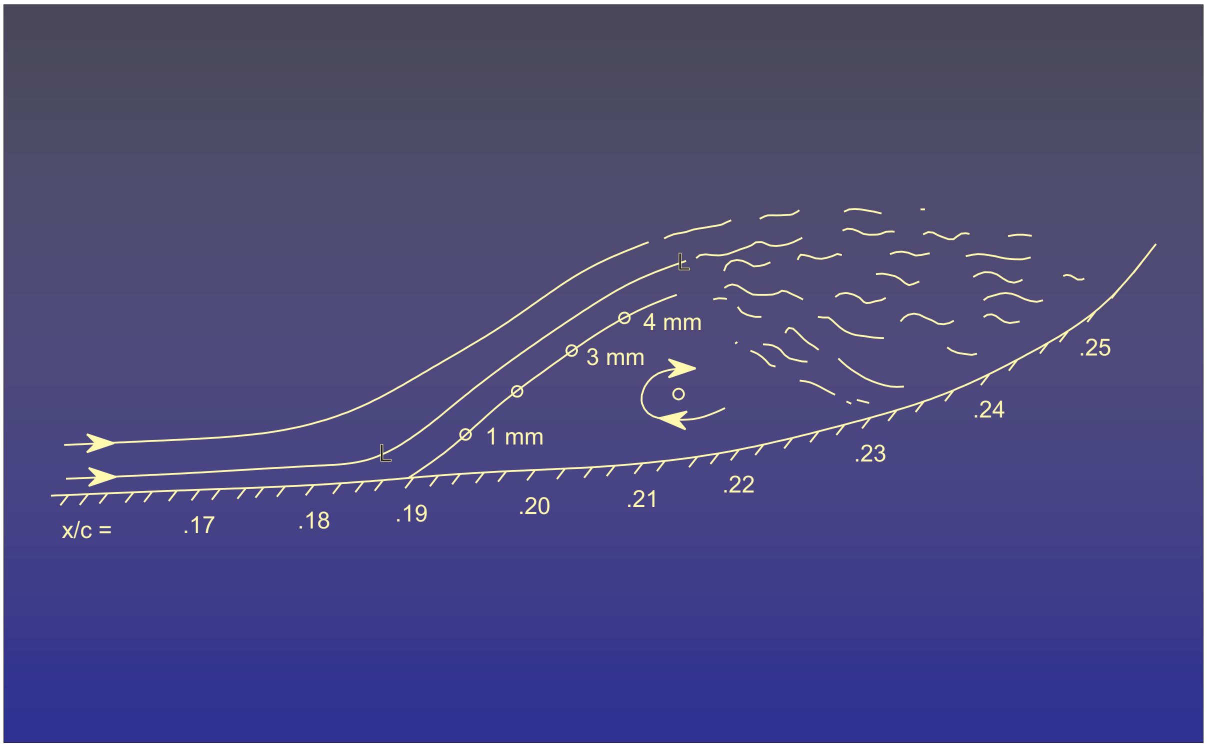

Figure 11. Observed laminar separation bubble. (not to scale)